Investigating the Mechanism for Copper Removal in Constructed Wetlands Using Batch Adsorption Isotherm Experiment

Stella Ban

ABSTRACT

This study investigated the adsorption behavior of copper (II) in anaerobic and aerobic conditions using soil and sand as substrates. The results showed that there was no significant difference in copper adsorption behavior between anaerobic and aerobic conditions when the soil was used as the substrate. The main mechanism of copper sorption was the electrostatic attraction between the sorbent and copper (II). In general, the soil had a higher surface area compared to sand, indicating a higher capacity for copper sorption. However, more experiments are needed to determine whether sand or soil is a better substrate for copper removal. Future directions include modifying the anaerobic environment to reach sulfide-reducing conditions, testing different types of clay for copper sorption, measuring the amount of pharmaceutical organic chemicals in soil, using phosphate buffer, and conducting more experiments at different concentration ranges. Overall, the study provides insights into the adsorption behavior of copper (II) in anaerobic and aerobic conditions and lays the groundwork for future research on soil and sand as substrates for copper removal. Analytical methods like Ion chromatography, Inductively coupled plasma mass spectrometry, FT-IR spectroscopy, Scanning electron microscope, and x-ray diffraction measurements are implanted to understand the chemical composition and surface morphology of the substrates.

KEYWORDS

Horizontal Levee, copper sorption, electrostatic attraction, sulfide-reducing conditions, SEM

INTRODUCTION

Copper is a naturally occurring trace element that is abundant in the Earth's crust and surface waters. Its presence in aquatic systems can be attributed to both natural and anthropogenic sources. Natural sources include geological deposits, volcanic activity, and weathering and erosion of rocks and soils (US EPA 2015). Anthropogenic sources of copper in aquatic systems include mining activities, agriculture, metal and electrical manufacturing, and algicide use (US EPA 2014). At low concentrations, copper is an essential nutrient, but at higher concentrations, it can be toxic to aquatic organisms. Copper can inhibit the growth of microorganisms that has an ecological role as primary decomposers, and it was widely used as an algicide (Flemming and Trevors 1989). According to an EPA report, approximately 350 tests were used to derive normalized LC50 values, representing 27 different genera of 15 species of invertebrates, 22 species of fish, and 1 amphibian species. The study found that invertebrates, in general, were more sensitive than fish and Species Mean Acute Values (SMAV) for copper ranged from 2.37 µg/L for the most sensitive species, *Daphnia pulicaria*, to 107,860 µg/L for the least sensitive species, *Notemigonus crysoleucas* (US EPA 2014). Additionally, the study has shown that concentrations of copper ranging from 1 to 8,000 µg/L have been shown to inhibit the growth of various freshwater plant species, including duckweed and green algae (US EPA 2014). As a result, reducing the levels of copper in aquatic systems through proper waste management and remediation efforts can play a crucial role in protecting aquatic organisms and maintaining the health of these ecosystems.

Constructed wetlands have emerged as an eco-friendly and cost-effective alternative to traditional physicochemical equipment and biological reactors used in wastewater treatment plants (Liang et al. 2017). Constructed wetlands have become a sustainable solution for water treatment, efficiently removing various pollutants, including heavy metals like copper, while also having the potential to act as carbon sinks and buffers for coastal cities facing sea level rise. Studies have shown that the constructed wetlands have very high efficiencies for metal removal including 75-78% for cadmium, chromium, and zinc, 84% for lead, and 55% for nickel (Sinicrope et al. 1992), and an excess of 80% removal from inflow to outflow (Knox et al. 2010). Constructed wetlands use several processes to remove metals, including sedimentation, flocculation, absorption, co-precipitation, cation and anion exchange, complexation,

precipitation, oxidation, reduction, microbiological activity, and plant uptake (Matagi et al. 1998 p. 199). Extensive research has focused on contaminant removal attributed to microbiological activity and plant uptake. For example, microbial processes like methylation could potentially affect metals' mobility, toxicity, and bioavailability (Kosolapov et al. 2004). Also, the sulfate-reducing bacteria can produce H_2S that is highly associated with copper, transforming copper from soluble phase to precipitate, and lowering its concentration in freshwater systems (Cecchetti et al. 2020). The constructed wetland has a high public acceptance and low costs which gives it great potential in treating reverse osmosis concentrates for future wastewater treatment plants (Cecchetti et al. 2022). Designing an absorption isotherm experiment is essential for understanding the underlying mechanism for wetland copper removal, which enables the possibility of making constructed wetlands immensely adaptable to all wastewater treatment plants, lowering their costs, and increasing overall efficiency.

The primary goal of this project is to identify the major mechanism of copper removal in constructed wetlands using an adsorption isotherm experiment. Two sub-questions will be investigated: 1) What is the efficiency of metal removal in anaerobic and aerobic environments, and how do they compare? 2) How does the efficiency of copper sorption compare between soil and sand substrates? The dominant mechanism will then be studied to achieve the greatest removal efficiency.

EXPERIMENTAL

General

Sodium Chloride (≥99.0 %) and MOPS buffer (≥97.0 %), were purchased from Fischer Scientific. Copper(II) Chloride (≥99.0 %) was purchased from Sigma-Aldrich. Ottawa Standard Sand(20-30 Mesh) was purchased from Spectrum Chemical. Sodium hydroxide (10N; Fischer Scientific) was used to adjust the pH of the solutions. All batches were prepared using distilled water from a Milli-Q deionized water generator.

Copper concentration in solution was analyzed using Agilent Technologies 7700 Series ICP-MS. Sulfate concentrations for liquid collected in anaerobic conditions were analyzed using Thermo Scientific Dionex ICS-1100. The chemical composition of sand and soil was analyzed by X-ray diffraction (XRD) composed with a PANalytical X'Pert Pro diffractometer equipped with a Co x-ray tube and the very fast X'Celerator. Surface morphology for the suspending clay particles and the remaining solids were analyzed by Zeiss EVO Variable Vacuum Instrument -10, the Scanning Electron Microscope (SEM). Python with the software Pycharm was used for statistical analysis.

Soil sample collection

The soil used in this experiment was collected from the top surface (0-8in) of a 0.7-ha experimental horizontal levee located in San Lorenzo, CA (37.67N by 122.16W) (Cecchetti et al., 2020). The horizontal levee had a gentle slope (1:30) and consisted of three granular media layers, arranged from the bottom to the top as gravel, coarse sand, varying loam topsoil layers, and vegetation. The topsoil layers consisted of different mixtures of fine clay loam excavated onsite and mixed with coarse sand (Cecchetti et al., 2020). The levee received a small fraction (<1%) of the secondary effluent from a conventional activated sludge wastewater treatment plant operated by the Oro Loma Sanitary (admin_ora_pmg, n.d.). Soil samples were collected all year and more often in the dry season (May-Aug) using an auger digger (Figure 11). They were sieved to 2mm, mixed well, and stored at -4°C before use. Soil moisture tests were conducted by calculating the percentage of mass lost before and after putting the weighted soil samples in a 105°C oven for 2 days. Soil moisture content on average is 12.56% (Table 2).

Soil sample characterization

The soil was vigorously mixed with distilled water (100ml) and sonicated for 20 minutes to facilitate the dispersion of soil particles. After 24 hours of settling, the clay suspension at the top and the bottom residue were collected separately by vacuum filtration. The clay portion was further treated with Glycol for 24 hours. The collected two portions were then subjected to XRD and SEM analysis to determine their mineralogical and morphological properties.

Batch Experiments

The experimental solution was prepared by mixing 0.017 g of NaCl, 0.021 g of MOPS buffer, pre-determined copper spike concentrations obtained from $CuCl_2$ ranging from 5 ppb to 700 ppb, and 100 mL of distilled water in a clean Nalgene plastic tube. The pH of the solution is adjusted to 6-7 with NaOH, and the ionic strength is 0.003 M. For each aerobic experiment, 10g of sand or soil sediments and 10 mL of the experimental solution were pulled into 50 mL polypropylene centrifuge tubes (triplicates) with cups open to achieve a solid-to-liquid ratio of 1 g/mL. For anaerobic experiments, transfer the polypropylene centrifuge tubes into a custom-built glove box that provides an air-tight environment. The "glove box" is constructed using a high-quality plastic bag and septums, and all joints are sealed with Teflon tape to ensure a secure seal (Figure 12). The centrifuge tubes were then placed on a rotating shaker and collect liquid samples from each vial at various time intervals ranging from 0 to 18 days using needles. The liquid samples were filtered through a 0.22 μm nylon membrane filter and prepared to be analyzed by ICP-MS.

RESULTS

Characterization of soil composition and surface morphology

Through X-ray diffraction (XRD), Fourier-transform infrared spectroscopy (FTIR) and Scanning Electron Microscope (SEM) analysis, the main mineral constituents of the sand and soil samples used in this experiment were identified. FT-IR diagrams were given in the appendix. The sand was found to primarily consist of Quartz, while the soil was composed of quartz, feldspar, montmorillonite clay, and some organic matter. Furthermore, Table. 1 presents the average particle sizes and surface area for each of the materials, where sand density is taken to be 1667 kg/m3 (Das and Sobhan 2014), montmorillonite clay density is found to be 2350 kg/m3 ("Montmorillonite Mineral Data" n.d.), and feldspar density is taken as 2560 kg/m3 (Alzahrani et al. 2022).

	Average Particle Size (μm)	Surface Area to Mass Ratio(m^2/kg)
Sand	**707**	**2.54**
Soil (Suspension Clay)	**0.2**	**6400**
Soil (Solid Residue)	**400**	**2.9**

Table 1. Sediments' average particle size and surface area to mass ratio.

XRD data

The mineral composition of soil is determined through XRD by measuring the distance between two crystal planes in a crystal lattice, known as the d-spacing. This is achieved using Bragg's Law equation: $n\lambda = 2d \cdot \sin\Theta$, where d represents the d-spacing, n is the order of diffraction, $\lambda(Co) = 1.79$ Å is the X-ray wavelength generated by the Cobalt source, and Θ is the angle at which the X-rays are diffracted from the crystal lattice planes.

Figure 2 presents the XRD analysis for the general composition of the bulk soil used in this experiment. The measured spectrum is represented by a red continuous curve, while the blue and black separated vertical lines correspond to the reference peaks for feldspar and quartz. Based on the XRD analysis, the soil was found to comprise approximately 79% quartz and 21% albite feldspar, with these two main components compared relative to each other based on the peak intensity.

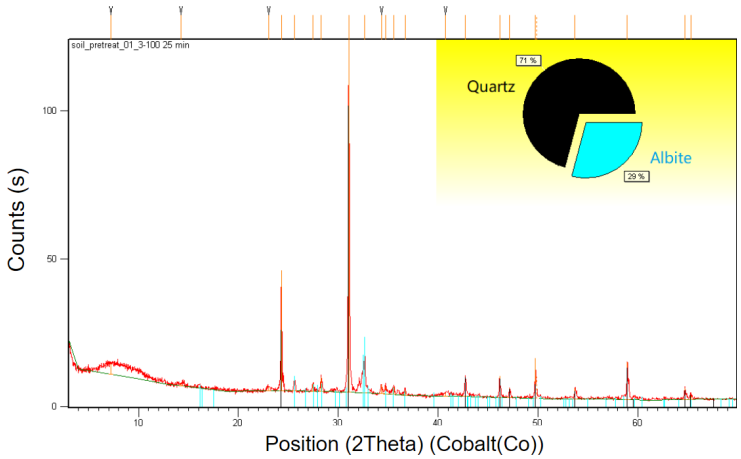

Figure 2. XRD diagram for bulk soil.

As shown in Figure 3, The clay's identity was determined to be a swelling clay belonging to the Montmorillonite family with chemical composition of $(K, Na)_{0.35}(Al, Mg, Fe)_{2\text{-}3}Si_{0.35}O_{10}(OH)_2 \cdot 4H_2O$ based on XRD analysis ("USGS OFR01-041: Clay Mineral Identification Flow Diagram" n.d.). The d_{001} spacing of the air-dried clay was measured to be 14.3Å, which is similar to the literature value of 14.2Å, and the d_{001} spacing increased to 16.5Å after glycol treatment, which is consistent with the literature value of 17Å for montmorillonite (Wenk and Bulakh, 2004).

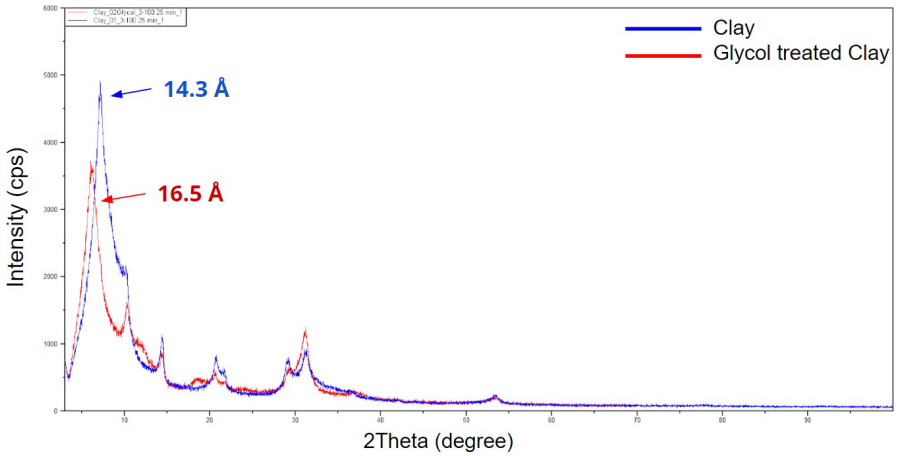

Figure 3. XRD diagram for homogeneous air-dried clay and 24 hours glycol-treated clay.

SEM data

The surface morphology of the montmorillonite clay particles appears to be predominantly homogeneous, with an average particle size of around 200nm as indicated on the right of Figure 4. There are also some larger, darker, and uneven surfaces present, which are likely composed of non-clay particles such as quartz debris, small fibers, and other impurities.
Scanning electron microscopy-energy dispersive X-ray analysis (SEM-EDX) was performed on an area containing only homogenous clay, revealing the relative composition of elements present indicated on the left of Figure 4. Through charge balance and mass balance calculations, the relative ratios of each element were recalculated and the relative composition of the clay was determined to be approximately O:Mg:Al:Si:K:Ca:Fe = 62.0:2.6:9.3:20.8:1.3:0.8:3.3, which is

similar to that of Montmorillonite (smectite) in terms of its chemical composition $(K, Na)_{0.35}(Al, Mg, Fe)_{2\text{-}3}Si_{0.35}O_{10}(OH)_2 \cdot 4H_2O$ (Wenk and Bulakh 2004). This supports that the clay presented in the soil is indeed montmorillonite.

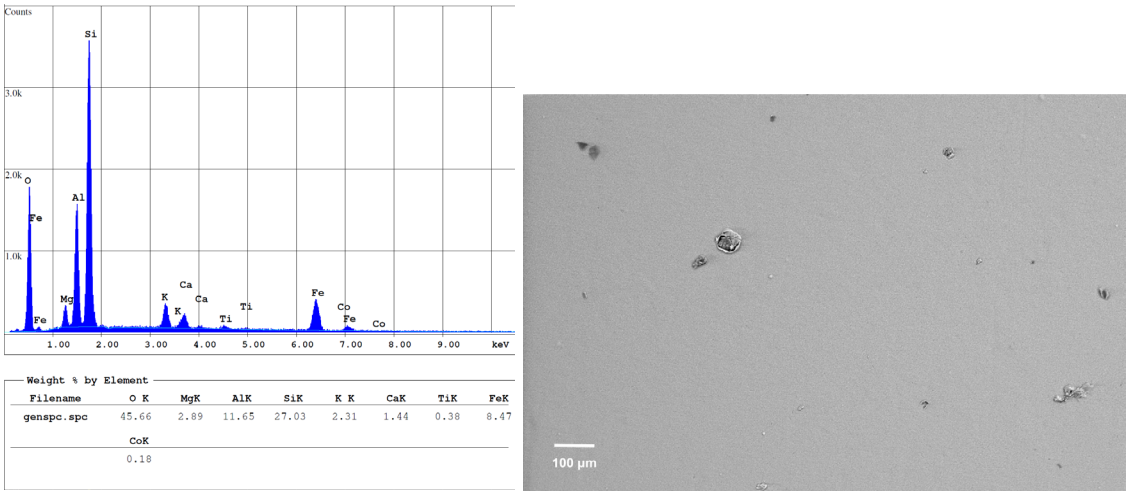

Figure 4. The right is the SEM photo of homogeneous clay, the left is the SEM-EDX analysis of chemical compositions for the clay.

After the sonication process, the soil residue was analyzed under SEM-EDX to identify individual rock types present. Most of the rocks identified were quartz and feldspars, which is consistent with the XRD data of the bulk soil and supports the previous measurement that the soil mainly consists of quartz and albite feldspar, with a relative composition of approximately 79% quartz and 21% albite feldspar. Additionally, small amounts of other minerals, including chromite, were also detected in the residue (Figure 5).

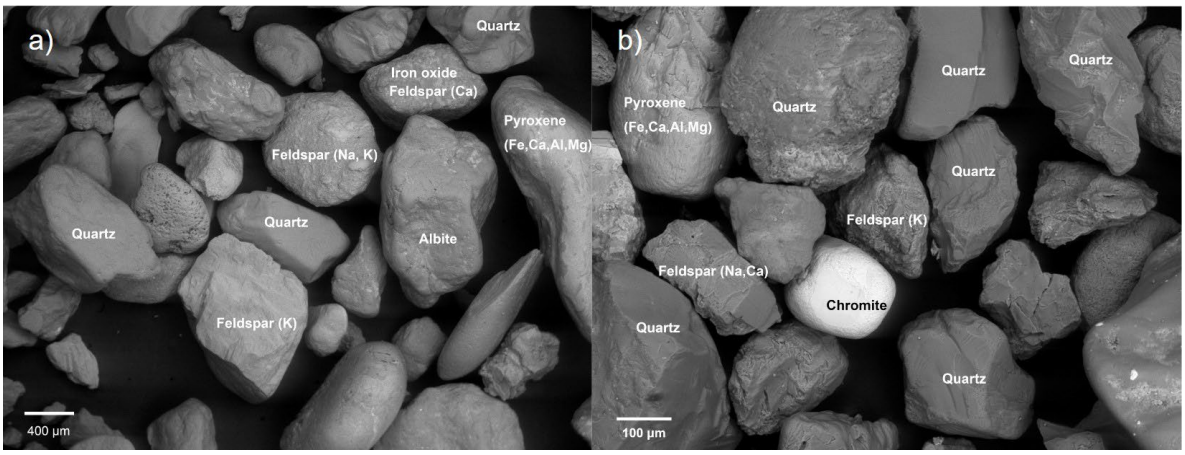

Figure 5. SEM photos of soil residue that settled after sonication. a) displays the residue under a reference of 400µm, and b) displays a zoomed-in view of the residue under a reference of 100µm.

Copper sorption on sand

Based on the data presented in Figure 6, it appears that sand exhibits rapid sorption of copper when subjected to spiked copper levels ranging from 5ppb to 49ppb, with the majority of the sorption occurring within the first 10 hours. Following this rapid sorption period, there is a slow equilibration process over the course of 94 hours, resulting in final copper concentrations of approximately 0-10ppb.

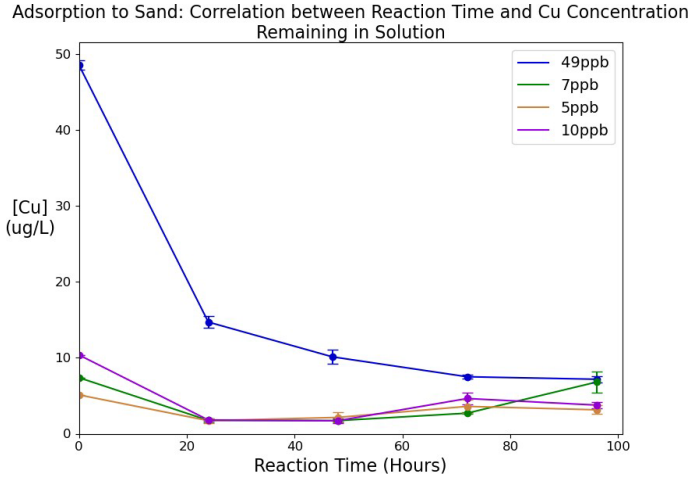

Figure 6. Copper adsorption onto sand with spiked copper concentrations 5, 7, 10, 49 ppb.

Copper sorption on soil

Based on Figure 7, the maximum amount of copper sorption occurs within the first 3 hours of contact between copper and soil, with equilibrium being reached within the first 26 hours for an initial spike of 70ppb, and between 70ppb and 20ppb for an initial spike of 700ppb of copper. The difference in sorption between aerobic and anaerobic conditions is not significant, as indicated by the overlapping error bars and the calculated p-values of 0.78 and 0.99 for batches carried out under aerobic and anaerobic conditions with copper spiked at 70ppb and 700ppb, respectively. Both p-values are larger than the significance level of 0.05, indicating that the difference is not statistically significant. The final equilibrium amount of copper does not significantly differ between the anaerobic and aerobic conditions, even when the reaction is allowed to continue for a longer period of time (Figure 14).

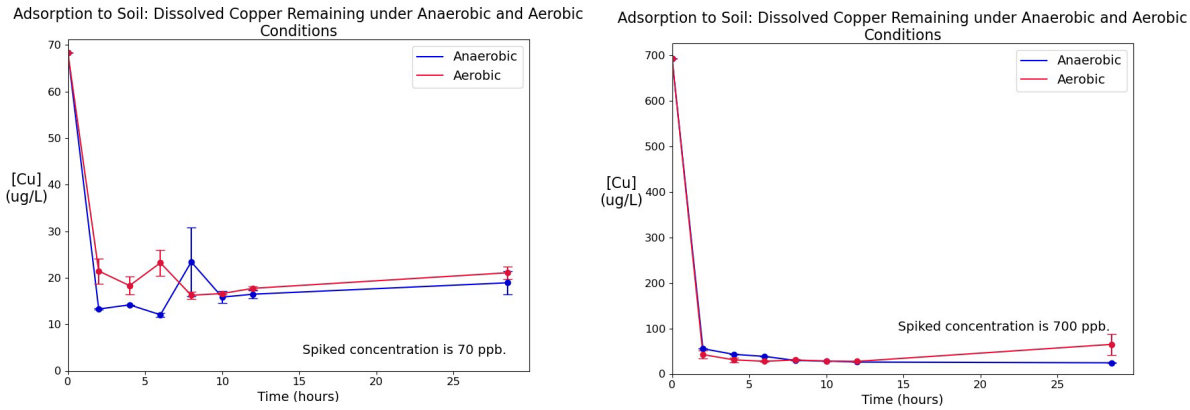

Figure 7. Copper sorption onto the soil. The left is spiked with 70 ppb of copper and the right is spiked with 700 ppb of copper.

Ion chromatography (IC) data indicates that the concentration of sulfate increased over a period of 17.5 days. Moreover, the average sulfate concentration was slightly higher for copper spiked at 700 ppb compared to that spiked at 70 ppb (Figure 8).

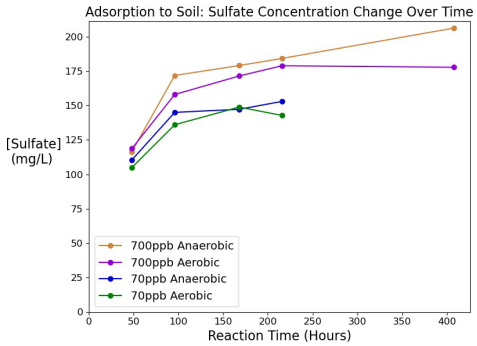

Figure 8. IC data indicating sulfate concentration over reaction time for soil in anaerobic conditions.

Effect of substrate for copper sorption

The dissociation constant (Kd) values for both sand and soil substrates in equilibrium conditions with 96 hours of reaction time show an increasing trend with spiked copper concentrations. When examining the spiked copper concentrations between 50 ppb and 70 ppb, the Kd values for sand and soil are similar. However, additional experiments and data points are required to draw a definitive conclusion (Figure 9).

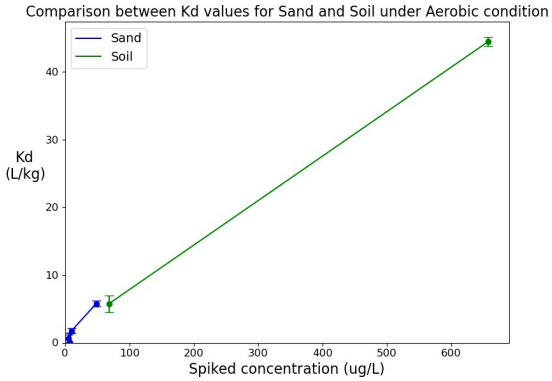

Figure 9. Dissociate constant against spiked copper concentrations.

DISCUSSION

Effect of anaerobic condition and aerobic conditions on copper sorption

Based on the data presented in Figure 7, there does not appear to be a significant difference in copper sorption between anaerobic and aerobic conditions when using soil as a substrate. One possible explanation for this is that, based on the ion chromatography data, the conditions necessary for sulfide reduction were not reached. Sulfide-reducing conditions refer to the presence of sulfate-reducing bacteria (SRB) in an anaerobic environment. These bacteria can oxidize organic matter or use other electron donors as a source of electrons to reduce sulfate to sulfide. The H_2S produced by the bacterial metabolic activity can react with metal ions to form water-insoluble metal sulfides, which play a crucial role in metal sulfide precipitation (Equation. 1). The precipitation of copper sulfide can increase copper sorption onto solid surfaces due to decreased copper solubility, increased surface area for sorption, and changes in redox conditions.

Given that the sulfide-reducing condition was not reached, it is reasonable to expect that there is not much difference between the aerobic and anaerobic conditions in terms of copper sorption.

Equation 1. The chemical equation for sulfide reduction and copper sulfide precipitation.

$$SO_4^{2-} + 8e + 9H^+ \xrightarrow[\text{Anoxic}]{\text{SRB}} HS^- + 4H_2O$$

$$HS^- + Cu^{2+} \longrightarrow CuS(s) + H^+$$

Effect of substrate on copper adsorption

The mechanism for copper sorption is predominantly believed to be electrostatic attraction forces between the positively charged copper(II) ions and the anionic surfaces of the substrate. For example, clay particles have largely silicon oxide tetrahedrons with negatively charged O- ions facing outwards (Figure 10). Similar silica oxide tetrahedral structures are observed on the mineral surfaces of feldspar and quartz as well ("Feldspars - all about the plagioclases and K-feldspars" n.d., "The Quartz Page: Quartz Structure" n.d.). Hence, electrostatic attraction is considered the major mechanism for copper adsorption for both sand and soil substrate in aerobic conditions. This highlights the importance of the surface area to mass ratio of each mineral, as substrates with a higher surface area are believed to have a higher rate of copper sorption. Table 1 shows that the surface area to mass ratio is the highest for clay, followed by solid residue for soil and quartz sand. However, it should be noted that the solid residue for soil consists of particles of various sizes, making it difficult to determine the average size and surface area to mass ratio for all particles. Furthermore, in order to obtain a more accurate measurement, additional treatments like an ash test may be required to quantify each portion of feldspar, quartz, clay, and organic matter that contributes to the total soil.

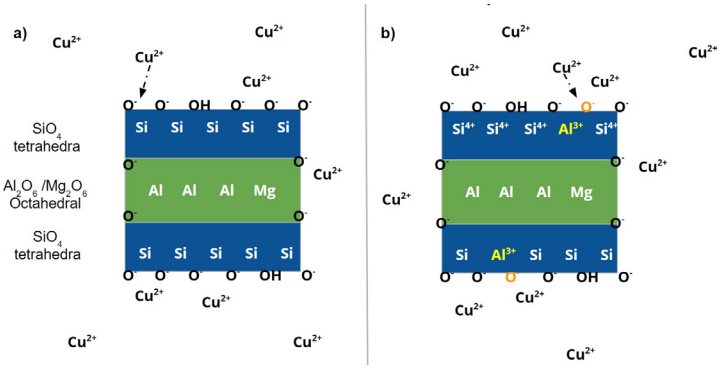

Figure 10. a) is an electrostatic attraction between clay surface and copper(II) ions. b) illustrate isomorphic substitution with an Al^{3+} ion substitute a Si^{4+} ion, increasing the net negative charge on the clay surface.

In both the sand and soil data presented in Figure 6 and Figure 7 and the appendix, it can be observed that at equilibrium, the rate of copper adsorption onto the adsorbent is equal to the rate of copper desorption back into the solution. Additionally, the amount of copper remaining in the solution is similar for all initial concentrations. This indicates that soil is an effective adsorbent for copper at high concentrations, and it can rapidly sorb copper from solutions with concentrations as high as 700 ppb (Figure 7). The fast equilibration process over time suggests that the adsorption sites on the substrate have not yet reached their saturation point, and once this point is reached, the rate of sorption may slow down. This implies that there are still available sites on the substrate that can adsorb more copper.

The experimental data in Figure 9 suggests that the Kd values for soil and sand are relatively similar in the range of 50 to 70 ppb of copper. However, further experiments are needed to collect additional data points to draw a conclusive conclusion.

Limitations and Future Directions

While this study found no significant difference in copper adsorption between anaerobic and aerobic conditions, the desired sulfide-reducing condition was not achieved in the anaerobic setup. Future research may focus on modifying the anaerobic environment by adding carbohydrates like lactose to act as electron donors for the microbes, potentially enabling the system to reach sulfide-reducing conditions. Such modifications could enhance the overall copper removal efficiency of the anaerobic setup. Alternative substrates, such as clays (e.g. Kaolinite and Illite), with varying numbers of hydrogen bonds in their inner layer, can be explored to investigate their adsorption properties. Expanding and non-expanding clays can be tested to determine if their differences in hydrogen bonds and particle size lead to variations in adsorption properties. Additionally, the study only measured copper adsorption at concentrations ranging from 0-700 ppb, and further experiments at concentrations between 70-700 can be helpful to fully understand the substrate's performance. Furthermore, an ash test can be carried out to determine the amount of organic carbons present in the soil, which can be complex with copper ions. Laser diffraction measurements can be performed to quantify the particle sizes of each type of mineral. Copper speciation calculations can be useful to determine the type of

copper present in the system. Phosphate buffer can be used to replace MOPS buffer, which can be helpful to prevent potential complexion between the sulfate group on the MOPS buffer and the copper ions. In conclusion, while the current study sheds light on the copper adsorption behavior in anaerobic and aerobic conditions using soil and sand as substrates, future studies could explore and optimize the use of different substrates and experimental conditions for copper removal.

CONCLUSION

In this study, we showed that there is no significant difference in copper adsorption behavior between anaerobic and aerobic conditions when soil is used as the substrate. The primary mechanism involved in copper sorption is the electrostatic attraction between the sorbent and the Copper (II) ions. Soil is mainly composed of quartz and albite feldspar with a relative ratio of 79% and 21%. The total surface area plays a significant role in the capacity for copper sorption, with soil having a higher surface area in general compared to sand. While this study provides valuable insights, more experiments need to be conducted to determine whether soil or sand is a better substrate for copper removal. It is also important to note that the hydrogen bond is a stronger force compared to Van der Waals (vdW) forces and electrostatic forces, which can have implications for the design of future copper removal technologies. Overall, this study sheds light on the complex interplay between substrate characteristics and copper sorption behavior, highlighting the need for further research in this field.

ASSOCIATED CONTENT

Literature articles cited in environmental science fields. This material is available free of charge via the Internet.

ACKNOWLEDGMENT

Appreciated Professor David L. Sedlak, and all the group members and lab managers in Sedlak's lab. Great help was been provided by peers in the lab.

REFERENCES

admin_ora_pmg. (n.d.). Horizontal Levee Project.

Alzahrani, A. M., E. S. R. Lasheen, and M. A. Rashwan. 2022. Relationship of Mineralogical Composition to Thermal Expansion, Spectral Reflectance, and Physico-Mechanical Aspects of Commercial Ornamental Granitic Rocks. Materials 15:2041.

Cecchetti, A. R., A. N. Stiegler, E. A. Gonthier, S. R. S. Bandaru, S. C. Fakra, L. Alvarez-Cohen, and D. L. Sedlak. 2022. Fate of Dissolved Nitrogen in a Horizontal Levee: Seasonal Fluctuations in Nitrate Removal Processes. Environmental Science & Technology 56:2770–2782.

Cecchetti, A. R., A. N. Stiegler, K. E. Graham, and D. L. Sedlak. 2020. The horizontal levee: a multi-benefit nature-based treatment system that improves water quality and protects coastal levees from the effects of sea level rise. Water Research X 7:100052.

Das, B. M., and K. Sobhan. 2014. Principles of Geotechnical Engineering, SI Edition. Cengage Learning.

Flemming, C. A., and J. T. Trevors. 1989. Copper toxicity and chemistry in the environment: a review. Water, Air, and Soil Pollution 44:143–158.

Knox, A. S., E. A. Nelson, N. V. Halverson, and J. B. Gladden. 2010. Long-Term Performance of a Constructed Wetland for Metal Removal. Soil and Sediment Contamination: An International Journal 19:667–685.

Kosolapov, D. B., P. Kuschk, M. B. Vainshtein, A. V. Vatsourina, A. Wießner, M. Kästner, and R. A. Müller. 2004. Microbial Processes of Heavy Metal Removal from Carbon-Deficient Effluents in Constructed Wetlands. Engineering in Life Sciences 4:403–411.

Liang, Y., H. Zhu, G. Bañuelos, B. Yan, Q. Zhou, X. Yu, and X. Cheng. 2017. Constructed wetlands for saline wastewater treatment: A review. Ecological Engineering 98:275–285.

Matagi, S. V., D. Swai, and R. Mugabe. 1998. A review of Heavy Metal Removal Mechanisms in wetlands. African Journal of Tropical Hydrobiology and Fisheries 8:13–25.

Montmorillonite Mineral Data. (n.d.). . http://webmineral.com/data/Montmorillonite.shtml#.ZDe3cHbML18.

Sinicrope, T. L., R. Langis, R. M. Gersberg, M. J. Busnardo, and J. B. Zedler. 1992. Metal removal by wetland mesocosms subjected to different hydroperiods. Ecological Engineering 1:309–322.

US EPA, O. 2014, February 11. Aquatic Life Criteria - Copper. Other Policies and Guidance. https://www.epa.gov/wqc/aquatic-life-criteria-copper.

US EPA, O. 2015, October 13. Lead and Copper Rule. Other Policies and Guidance. https://www.epa.gov/dwreginfo/lead-and-copper-rule.

USGS OFR01-041: Clay Mineral Identification Flow Diagram. (n.d.). . https://pubs.usgs.gov/of/2001/of01-041/htmldocs/flow/index.htm.

Wenk, H.-R., and A. G. Bulakh. 2004. Minerals: their constitution and origin. Cambridge University Press, Cambridge ; New York.

SUPPLEMENTAL INFORMATION

Moisture Content: Soil collected in cell K 0-8in depth					
	Wet Soil Mass (g)	**Weight Boat Mass (g)**	**Dried Total Mass (g)**	**Dried Soil Mass (g)**	**Moisture content (%)**
Trial 1	1.5461	2.2482	3.6029	1.3547	12.38%
Trial 2	1.6472	2.2547	3.7106	1.4559	11.61%
Trial 3	1.4824	2.2516	3.5549	1.3033	12.08%
Trial 4	1.4354	2.2674	3.5212	1.2538	12.65%
Trial 5	1.3609	2.1845	3.3646	1.1801	13.29%
Trial 6	1.5817	2.2198	3.5907	1.3709	13.33%
				Average	**12.56%**

Table 2. Soil moisture content test.

Figure 11. Auger digger used for soil sampling.

Figure 12. Homemade glove-box.

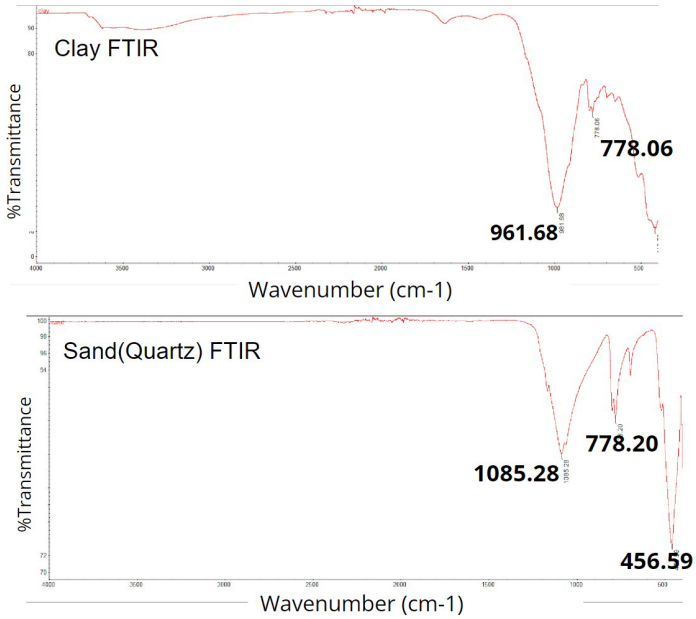

Figure 13. FT-IR diagram for clay and sand.

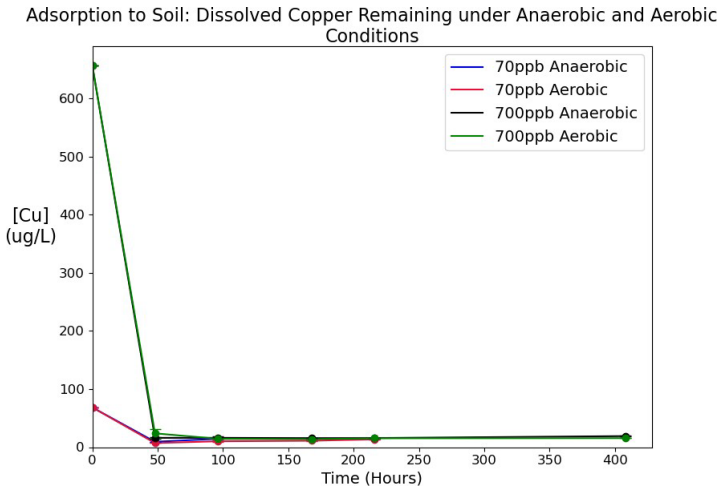

Figure 14. Copper adsorption to Soil with longer reaction time in days.